IEEE Access
Multidisciplinary | Rapid Review | Open Access Journal

Received 13 August 2023, accepted 6 September 2023, date of publication 11 September 2023,
date of current version 15 September 2023.

Digital Object Identifier 10.1109/ACCESS.2023.3313931

RESEARCH ARTICLE

Performance Analysis of MIMO-EGC System for the Underwater Vertical Wireless Optical Communication Link

C. S. SAVIDHAN SHETTY[1], (Student Member, IEEE), RAMAVATH PRASAD NAIK[2], U. SHRIPATHI ACHARYA[1], (Senior Member, IEEE), AND WAN-YOUNG CHUNG[3], (Senior Member, IEEE)

[1]Department of Electronics and Communication Engineering, National Institute of Technology Karnataka, Surathkal 575025, India
[2]Department of Electronics and Communication Engineering, National Institute of Technology Rourkela, Rourkela 769008, India
[3]Department of Electronic Engineering, Pukyong National University, Busan 48513, South Korea

Corresponding authors: C. S. Savidhan Shetty (savidhan.cs@gmail.com) and Wan-Young Chung (wychung@pknu.ac.kr)

The work of C. S. Savidhan Shetty work was supported by the Ph.D. Fellowship granted by the Ministry of Education, Government of India. This work was supported by a Research Grant funded by the National Research Foundation (NRF) of Korea under Grant 2019R1A2C1089139.

ABSTRACT In this paper, we have investigated the performance of an underwater vertical wireless optical communication (UVWOC) link employing multiple input-multiple output (MIMO) operating in conjunction with equal gain combing (EGC) techniques perturbed by weak and strong turbulence in the presence of pointing errors and attenuation losses. Vertical underwater turbulence, which varies from layer to layer due to temperature and salinity variation connected to depth, is modeled using hyperbolic tangent log-normal (HTLN) distribution in the case of weak underwater turbulence and gamma-gamma (GG) distribution in the case of strong underwater turbulence. Novel closed-form expressions quantifying the average bit error rate (BER) have been derived for the UVWOC MIMO EGC system for weak and strong turbulence regimes. The expression for the average BER associated with the UVWOC link for different values of pointing error, differing vertical layer depth, modulation types, and differing numbers of sources and detectors have been determined. In addition, closed-form expressions for the outage probability (OP) and ergodic channel capacity (ECC) have been derived for the UVWOC MIMO EGC system. The accuracy of all closed-form expressions derived in the paper has been verified using Monte Carlo simulations.

INDEX TERMS Underwater vertical wireless optical communication (UVWOC), hyperbolic tangent log-normal (HTLN) distribution, average BER, outage probability (OP), ergodic channel capacity (ECC), equal gain combining (EGC).

I. INTRODUCTION

There has been a great deal of interest in investigating, evaluating, and designing underwater wireless optical communication (UWOC) systems in the recent past. This is due to the fact that optical wireless communication systems can enable high transmission rates and reliable communication in oceanic channels over short distances [1], [2], [3]. Beam absorption, pointing errors, and underwater turbulence are the major impediments affecting UWOC systems. The intensity level is reduced by absorption and scattering, causing deviation of the beam from the intended line of sight path. The propagating optical beam will be attenuated due to the combined effect of absorption and scattering. The effects of beam attenuation are minimized by employing an optical source operating in the wavelength range of 400-530 nm [4], [5]. The effect of Beam spread functions for different types of water is studied in the literature [37].

The turbulence of the oceanic medium causes variations in the intensity of the propagating beam as light travels

The associate editor coordinating the review of this manuscript and approving it for publication was Tianhua Xu.

inside water. This underwater turbulence is modeled using log-normal distribution in a weak turbulence regime and gamma-gamma (GG) distribution in a strong turbulence regime [3], [32], [33], [38]. In most of the literature, a link is assumed to be horizontal in which case the turbulence value can be assumed as constant over the entire length of the link. In the case of vertical optical links, temperature and salinity variations can be observed across the length of the link. This results in the formation of non-identical vertical layers [6], [7]. These multiple non-identical vertical layers (Each vertical layer with different turbulence) are modeled using cascaded log-normal and gamma-gamma turbulence for weak and strong regimes, respectively [8], [9]. The low complexity HTLN distribution is used as an alternative to log-normal distribution to model vertical link turbulence in case of weak regimes [15]. In this paper, we have assumed the link to be vertical and used HTLN distribution and cascaded GG distribution for channel modeling with respect to weak and strong turbulence regimes. Pointing errors is another limitation that degrades the performance of UWOC systems. This is due to a misalignment between the source and detector, which results in the transmitted light beam deviating from the center line of the receiver. The performance of underwater links with pointing errors have been studied in literature [10], [11]. Due to the combined effect of vertical underwater turbulence, pointing error, and attenuation losses, the performance of the UVWOC system deteriorates. The performance of the communication system can be improved by using diversity techniques. Transmit diversity, receive diversity, and multiple input multiple output (MIMO) schemes are some of the methods that have been employed to improve the performance of underwater wireless optical communication links [12], [13], [14]. Equal Gain Combining (EGC) is often preferred at the receiver side due to its significantly simpler structure and comparable performance to maximum ratio combining [8], [12], [16], [34], [35]. In this paper, we have used the MIMO-EGC system model to improve the performance of vertical links.

A. MOTIVATION

A study of relevant literature reveals that most of the research work carried out to date has addressed the problem of light beam propagation through vertical underwater links comprising of K vertical layers where a single source and detector have been employed. Thus, most of the study and analysis have been focused on single input, single output systems. Such systems are particularly vulnerable to the impact of pointing errors [7]. The research work reported in this paper has been driven by the desire to address this limitation. In the literature [15], channel models for vertical links were derived by the author, taking into consideration the effect of pointing errors, with a specific focus on the weak turbulence regime. Different schemes, such as receive diversity with selection combining and maximum ratio combining, were explored [15]. Drawing upon the encouraging results of prior research, a novel approach has been adopted in this paper, where MIMO EGC has been employed for vertical links with K vertical layers. Notably, this marks the first instance of channel modeling for the MIMO EGC system in the context of underwater vertical links. In Table 1, we have provided existing work related to the underwater wireless optical vertical link.

TABLE 1. Existing work on vertical link underwater wireless optical communication.

Reference	Authors Contributions
[7]	Proposed channel modeling of vertical link underwater turbulence. Derived closed-form expressions for average BER and ergodic channel capacity (ECC) for single input single output (SISO) vertical link without considering the pointing error effect.
[15]	Derived closed form expression for selection combining (SC) and maximum-ratio combining (MRC) receive diversity schemes for vertical link quantifying average BER, ECC, and outage probability (OP) considering pointing error effect in weak turbulence.
[30]	Derived closed form average BER expression for SISO vertical link for strong turbulence with pointing error.
[28]	Derived closed-form outage probability expression and diversity gain for MIMO- EGC vertical link for weak turbulence without considering pointing error effect.
[31]	Derived closed-form outage probability expression for SISO vertical link for weak turbulence considering pointing error effect.

The contributions made by this research paper are enumerated below:

- Unified combined probability density function (PDF) and cumulative distribution function (CDF) have been derived for the MIMO- EGC- UVWOC link perturbed by weak and strong turbulence. The effects of pointing error and attenuation losses have been taken into account while deriving these expressions.
- Novel closed-form expressions quantifying average bit error rate (BER), outage probability (OP), and ergodic channel capacity (ECC) have been derived separately for weak turbulence and strong turbulence regimes.
- The accuracy of the analytical expressions derived in the paper has been verified using Monte-Carlo simulations.

The remainder of the paper is organized as follows. The system model of UVWOC MIMO EGC has been presented in Section II. The individual channel models for weak and strong turbulence, including pointing errors and attenuation losses, have been presented in Section III. The average BER, OP, and ECC analysis of the UVWOC MIMO EGC system is described in Section IV. We have included a discussion of the relevance and significance of the results obtained in this paper in Section V. The paper has been concluded in Section VI with a summary of the research results reported. Notations and parameters used in paper represented in Table 2.

II. SYSTEM MODEL

Consider a UVWOC system model as shown in Fig. 1. The system consists of M LASER sources and N photo-detectors.

TABLE 2. Parameters and notations used in paper.

M	Number of Transmitters
N	Number of Receivers
K	Number of vertical layers
(α_k,β_k)	Gamma-gamma parameters of k^{th} layer.
I_a	Attenuation coefficient
A_0	Fraction of collected power at the receiver when displacement is zero
L	MN
g	Pointing error parameter.

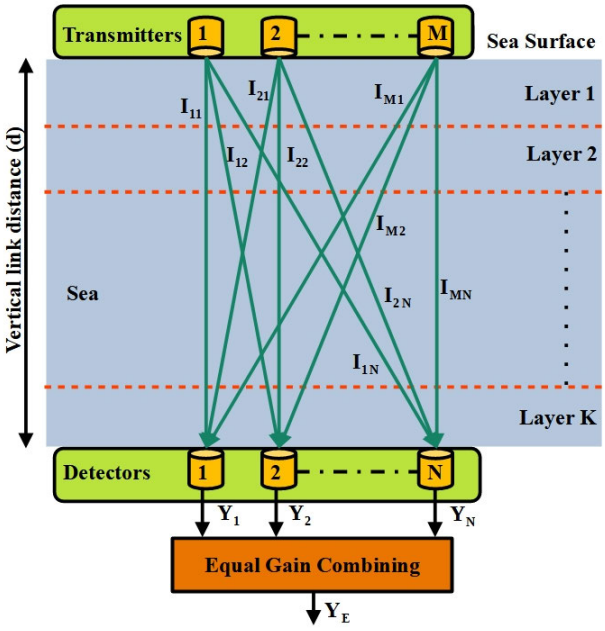

FIGURE 1. UVWOC MIMO EGC system.

The data received at the j^{th} photo-detector is given by [16],

$$Y_j = \frac{\eta}{MN}\sum_{i=1}^{M} I_{i,j}x + v_j, \quad j = 1, 2, \cdots N \tag{1}$$

where η is the responsivity of the photo-detector, $I_{i,j}$ is the fading coefficient of i^{th} LASER source to j^{th} photo-detector, x is the transmitted data, and v_j is additive white Gaussian noise at each receiver with zero mean and variance $\sigma_j^2 = \sigma^2/N$. We have assumed that the responsivities of all photo-detectors are equal. The output of the equal gain combiner at the receiving end is given by

$$Y_E = \sum_{j=1}^{N} Y_j = \frac{\eta}{MN} I_E x + v_E \tag{2}$$

where $I_E = \sum_{i=1}^{M}\sum_{j=1}^{N} I_{i,j}$ and $v_E = \sum_{j=1}^{N} v_j$. The signal-to-noise (SNR) ratio of equal gain combined received signal is given by

$$\gamma_E = \frac{\eta^2 I_E^2 E_x}{M^2N^2\sigma^2} = \frac{\bar{\gamma} I_E^2}{M^2N^2} \tag{3}$$

where E_x is energy of transmitted signal and $\bar{\gamma} = \frac{\eta^2 E_x}{\sigma^2}$ is average SNR.

III. CHANNEL MODELS

In this section, we have derived the combined PDF and CDF of the channel for the proposed system. The combined fading coefficient after equal gain combining is given by [8]

$$I_E = \sum_{i=1}^{M}\sum_{j=1}^{N} I_{i,j} \tag{4}$$

where $I_{i,j}$ is the fading coefficient associated with each received signal. It is computed as the product of the individual fading coefficients associated with attenuation I_a, pointing error $I_{p_{i,j}}$ and turbulence of underwater medium $I_{t_{i,j}}$, i.e., $I_{i,j} = I_a I_{t_{i,j}} I_{p_{i,j}}$.

A. ATTENUATION CHANNEL MODEL

The attenuation of the underwater channel by considering both absorption losses and scattering losses is given by [3]

$$I_a = \exp\left(-dC(\lambda)\right) \tag{5}$$

where $C(\lambda)$ is wavelength (λ) dependent extinction coefficient and d is the vertical link distance between source and detector.

B. VERTICAL LINK TURBULENCE CHANNEL MODEL

The PDF of fading coefficient associated with the propagating light beam in the case of UVWOC links under conditions of weak and strong turbulence has been specified in the following paragraphs.

1) WEAK TURBULENCE

It has been shown that in the case of a weak turbulence regime, the PDF of fading coefficient associated with the propagating light beam will follow a log-normal distribution [7]. Under these conditions, the PDF of the fading coefficient considering K non-identical vertical layers is described by [7]

$$f_{I_{t_{i,j}}}\left(I_{t_{i,j}}\right) = \frac{1}{2I_{t_{i,j}}\sqrt{2\pi\sigma_t^2}} \exp\left(-\frac{\left(\ln\left(I_{t_{i,j}}\right) - 2\mu_t\right)^2}{8\sigma_t^2}\right) \tag{6}$$

In this equation, the total log-amplitude mean and variance are $\mu_t = \sum_{k=1}^{K}\mu_{x_k}$ and $\sigma_t^2 = \sum_{k=1}^{K}\sigma_{x_k}^2$ respectively.

2) STRONG TURBULENCE

It has been shown that under strong turbulence conditions, the fading coefficient associated with propagating light beam will follow the gamma-gamma (GG) distribution. This density function considering K non-identical vertical layers is given by (7), as shown at the bottom of the next page, [7].

In (7), α_k and β_k are the parameters related to GG for the k^{th} layer, $\{\alpha_k - 1\}_{k=1}^{K} = \{\alpha_1 - 1, \alpha_2 - 1 \cdots, \alpha_K - 1\}$, $\{\beta_k - 1\}_{k=1}^{K} = \{\beta_1 - 1, \beta_2 - 1 \cdots, \beta_K - 1\}$, $A_{\alpha\beta} = \prod_{k=1}^{K}\alpha_k\beta_k$ and $B_{\alpha\beta} = \prod_{k=1}^{K}\Gamma(\alpha_k)\Gamma(\beta_k)$.

C. POINTING ERRORS CHANNEL MODEL

The parameter associated with misalignment between the source and detector is a pointing error. The pointing error fading coefficient of the overall channel comprising of K layers is given by [17]

$$I_{p_{i,j}} \approx A_0 \exp\left(-\frac{2R^2}{\omega_{zeq}^2}\right), \quad R \geq 0 \tag{8}$$

where R denotes the Rayleigh distributed random displacement variable, A_0 is the fraction of the collected power at $R = 0$ and ω_{Zeq} is the equivalent beam width.

D. COMBINED CHANNEL MODEL

In this section we derived combined PDF and CDF of fading coefficient associated with equal gain combining by considering the attenuation channel model, pointing error model, HTLN distribution in case of weak turbulence, and GG distribution for strong turbulence. The combined fading coefficient after equal gain combining, I_E can be expressed by using an approximation employed in [18, Eq. (12)] and given by

$$I_E = I_a S_1 S_2 \tag{9}$$

where $S_1 = \sum_{i=1}^{M}\sum_{j=1}^{N} I_{t_{i,j}}$ and $S_2 = \frac{1}{MN}\sum_{i=1}^{M}\sum_{j=1}^{N} I_{p_{i,j}}$. The PDF of variable S_2 is given by [18, Eq. (23)]

$$f_{S_2}(S_2) = \frac{(-1)^{L-1}(L)^L g^L}{S_2 2^L \Gamma(L)} \ln^{L-1}\left(\frac{S_2}{FA_0}\right)\left(\frac{S_2}{FA_0}\right)^{\frac{Lg}{2}}, \quad 0 \leq S_2 \leq FA_0 \tag{10}$$

where pointing error parameter $g = \frac{w_{zeq}^2}{2\sigma_s^2}$, $L = MN$ and $F = \frac{(2+gL)^L}{L^L g^{L-1}(2+g)}$.

1) COMBINED PDF

The PDF of the combined fading coefficient after EGC is given by [17]

$$f_{I_E}(I_E) = \int_{\frac{I_E}{FA_0 I_a}}^{\infty} \frac{1}{S_1 I_a} f_{S_2}\left(\frac{I_E}{S_1 I_a}\right) f_{S_1}(S_1) dS_1 \tag{11}$$

a: WEAK TURBULENCE

The PDF of the variable S_1 in case of weak turbulence will follow the log-normal distribution and is given by [4]

$$f_{S_1}(S_1) = \frac{1}{2S_1\sqrt{2\pi\sigma_E^2}} \exp\left(-\frac{(\ln(S_1) - 2\mu_E)^2}{8\sigma_E^2}\right) \tag{12}$$

where EGC mean $\mu_E = \frac{1}{2}\ln(L) - \frac{1}{4}\ln\left(1 + \frac{\exp(4\sigma_l^2)-1}{L}\right)$ and EGC variance $\sigma_E^2 = \frac{1}{4}\ln\left(1 + \frac{\exp(4\sigma_l^2)-1}{L}\right)$. The log-normal distribution in (12) can be represented by HTLN distribution for mathematical simplification and is given by [8]

$$f_{S_1}(S_1) = b\exp(2a) S_1^{b-1} G_{1,1}^{1,1}\left(\exp(2\,a)\, S_1^b \middle| \begin{matrix} -1 \\ 0 \end{matrix}\right) \tag{13}$$

where a and b are HTLN distribution parameters.

By substituting (13) in (11), the combined PDF in case of weak turbulence can be obtained in (14), as shown at the bottom of the page.

In (14), assume $\mathscr{Q} = -\ln\left(\frac{I_E}{FI_a S_1 A_0}\right)$ and integrating it by using Gauss-Laguerre quadrature formula for $'NN'$ sample points we get [29]

$$f_{I_E}(I_E) = \sum_{kk=1}^{NN} \mathscr{A}\mathscr{B} I_E^{b-1} \mathscr{E}(-\mathscr{Q})^{L-1} H_{kk} t_{kk}^{0.5} \times (-t_{kk})^{L-1} G_{1,1}^{1,1}\left(I_E^b \mathscr{C}\exp(t_{kk} b) \middle| \begin{matrix} -1 \\ 0 \end{matrix}\right) \tag{15}$$

where $\mathscr{A} = \frac{(-1)^{L-1}(L)^L g^L b\exp(2a)}{2^L\Gamma(L)}$, $\mathscr{B} = \frac{1}{(FA_0 I_a)^b}$, $\mathscr{C} = \frac{\exp(2a)}{(FA_0 I_a)^b}$, $\mathscr{E} = \exp\left(t_{kk}\left(1 + b - \frac{Lg}{2}\right)\right)$, t_{kk} are abcissae and H_{kk} are weight coefficients for the Gauss-Laguerre quadrature. The combined PDF in terms of SNR by change of variable $I_E = \frac{MN\sqrt{\gamma_E}}{\sqrt{\bar{\gamma}}}$ in (15) is given by

$$f_{\gamma_E}(\gamma_E) = \sum_{kk=1}^{NN} \frac{\mathscr{A}\mathscr{E} L^b H_{kk} t_{kk}^{0.5}(-t_{kk})^{L-1}\gamma_E^{(\frac{b}{2}-1)}}{2(\bar{\gamma})^{\frac{b}{2}}(FA_0 I_a)^b} \times G_{1,1}^{1,1}\left(\mathscr{Z}\middle| \begin{matrix} -1 \\ 0 \end{matrix}\right) \tag{16}$$

where $\mathscr{Z} = \left(\frac{L\sqrt{\gamma_E}}{\sqrt{\bar{\gamma}}}\right)^b \mathscr{C}\exp(-t_{kk} b)$.

b: STRONG TURBULENCE

The PDF of variable S_1 under the condition of strong turbulence regime will follow gamma-gamma distribution and is given by (17), as shown at the bottom of the next page [7], [19]

In (17), $\alpha_{E_k} = L\alpha_k + (L-1)\frac{-0.127 - 0.95\alpha_k - 0.0058\beta_k}{1 + 0.00124\alpha_k + 0.98\beta_k}$, $\{\alpha_{E_k} - 1\}_{k=1}^K = \{\alpha_{E_1} - 1, \alpha_{E_2} - 1 \cdots, \alpha_{E_K} - 1\}$, $\{\beta_{E_k} - 1\}_{k=1}^K = \{\beta_{E_1} - 1, \beta_{E_2} - 1 \cdots, \beta_{E_K} - 1\}$, $\beta_{E_k} = L\beta_k$, $A_E = \prod_{k=1}^K (\alpha_{E_k}\beta_{E_k})$ and $B_E = \prod_{k=1}^K (\Gamma(\alpha_{E_k})\Gamma(\beta_{E_k}))$.

$$f_{I_{t_{i,j}}}(I_{t_{i,j}}) = \frac{A_{\alpha\beta}}{B_{\alpha\beta}} G_{0,2K}^{2\,K,0}\left(A_{\alpha\beta} I_{t_{i,j}} \middle| \begin{matrix} - \\ \{\alpha_k - 1\}_{k=1}^K, \{\beta_k - 1\}_{k=1}^K \end{matrix}\right) \tag{7}$$

$$f_{I_E}(I_E) = \int_{\frac{I_E}{FA_0 I_a}}^{\infty} \frac{(-1)^{L-1}(L)^L g^L}{I_E 2^L\Gamma(L)} \ln^{L-1}\left(\frac{I_E}{FI_a S_1 A_0}\right)\left(\frac{I_E}{FI_a S_1 A_0}\right)^{\frac{Lg}{2}} S_1^{b-1} G_{1,1}^{1,1}\left(\exp(2\,a)\, S_1^b \middle| \begin{matrix} -1 \\ 0 \end{matrix}\right) dS_1 \tag{14}$$

By substituting (17) in (11) and integrating it in a similar way as in (14) the combined PDF of MIMO UVWOC EGC for strong turbulence is obtained in (18), as shown at the bottom of the page.

In (18), $\mathscr{A}_1 = \frac{(-1)^{L-1}(L)^L g^L A_E}{2^L \Gamma(L) F I_a A_0 B_E}$, $\mathscr{C}_1 = \frac{A_E}{F A_0 I_a}$, $\mathscr{E}_1 = \exp\left(t_{kk}\left(2 - \frac{Lg}{2}\right)\right)$ and $\mathscr{Z}_1 = \frac{I_E \mathscr{C}_1 \exp(t_{kk})}{L}$.

The combined PDF in terms of SNR by change of variable as in (16) can be obtained in (19), as shown at the bottom of the page.

In (19), $\mathscr{Z}_2 = \frac{\sqrt{\gamma_E}}{\sqrt{\bar{\gamma}}} \mathscr{C}_1 \exp(t_{kk})$.

2) COMBINED CDF

The combined CDF of MIMO UVWOC EGC system is given by

$$F_{\gamma_E}(\gamma_E) = \int_0^{\gamma_E} f_{\gamma_E}(\gamma_E)\, d\gamma_E \tag{20}$$

a: WEAK TURBULENCE

By substituting (16) in (20) and integrating it using formula in [20, Eq. (07.34.21.0084.01)] we get the combined PDF for weak turbulence as

$$F_{\gamma_E}(\gamma_E) = \sum_{kk=1}^{NN} \frac{\mathscr{A}\mathscr{E} L^b H_{kk} t_{kk}^{0.5} (-t_{kk})^{L-1} \gamma_E^{\frac{b}{2}}}{\pi b (\bar{\gamma})^{\frac{b}{2}} (F A_0 I_a)^b} \times G_{2+b,2+b}^{2,2+b}\left(\mathscr{W}^2 \gamma_E^b \middle| \begin{matrix} \frac{2i-b}{2b}, -0.5, 0 \\ 0, 0.5, \frac{2i-b-2}{2b} \end{matrix}\right) \tag{21}$$

where $i = 1, \cdots, b$ and $\mathscr{W} = \frac{L^b \mathscr{C} \exp(t_{kk} b)}{\bar{\gamma}^{\frac{b}{2}}}$.

b: STRONG TURBULENCE

By substituting (19) in (20) and integrating it [20, Eq. (07.34.21.0084.01)] the combined CDF for strong turbulence can be written as

$$F_{\gamma_E}(\gamma_E) = \sum_{kk=1}^{NN} \frac{\mathscr{A}_1 \mathscr{E}_1 2^u H_{kk} t_{kk}^{0.5} (-t_{kk})^{L-1} \sqrt{\gamma_E}}{2(2\pi)^K \sqrt{\bar{\gamma}}} \times G_{1,4K+1}^{4K,1}\left(\frac{\mathscr{W}_1^2 \gamma_E}{2^{4K}} \middle| \begin{matrix} 0.5 \\ \mathscr{O}, -0.5 \end{matrix}\right) \tag{22}$$

TABLE 3. OOK and BPSK modulation parameters.

Modulation Scheme	δ	p	q
OOK	1	0.5	0.5
BPSK	1	0.5	1

where $u = \sum_{k=1}^{K} \alpha_{E_k} + \beta_{E_k} - 3K + 1$, $\mathscr{W}_1 = \frac{\mathscr{C}_1 \exp(t_{kk})}{\sqrt{\bar{\gamma}}}$ and $\mathscr{O} = \frac{\{\alpha_{E_k}-1\}_{k=1}^K}{2}, \frac{\{\alpha_{E_k}\}_{k=1}^K}{2}, \frac{\{\beta_{E_k}-1\}_{k=1}^K}{2}, \frac{\{\beta_{E_k}\}_{k=1}^K}{2}$.

IV. PERFORMANCE ANALYSIS

In this section, we derive closed-form expressions for the average bit error rate (BER), outage probability (OP), and ergodic channel capacity (ECC) of the UVWOC MIMO EGC system.

A. AVERAGE BER

The average BER of the UVWOC MIMO EGC system is given by [9], [21]

$$P_E = \frac{\delta q^p}{2\Gamma(p)} \int_0^{\infty} e^{-q\gamma_E} \gamma_E^{p-1} F_{\gamma_E}(\gamma_E) d\gamma_E \tag{23}$$

where δ, p, and q are parameters related to different modulation techniques and corresponding values of these parameters for on-off keying (OOK) and binary phase shift keying (BPSK) modulations are shown in Table 3.

1) WEAK TURBULENCE

The average BER in case of weak turbulence is obtained by substituting (21) in (23) and given by

$$P_E = \frac{\delta q^p}{2\Gamma(p)} \int_0^{\infty} e^{-q\gamma_E} \gamma_E^{p-1} \times \sum_{kk=1}^{NN} \frac{\mathscr{A}\mathscr{E}(MN)^b H_{kk} t_{kk}^{0.5} (-t_{kk})^{L-1} \gamma_E^{\frac{b}{2}}}{\pi b (\bar{\gamma})^{\frac{b}{2}} (F A_0 I_a)^b} \times G_{2+b,2+b}^{2,2+b}\left(\mathscr{W}^2 \gamma_E^b \middle| \begin{matrix} \frac{2i-b}{2b}, -0.5, 0 \\ 0, 0.5, \frac{2i-b-2}{2b} \end{matrix}\right) d\gamma_E \tag{24}$$

$$f_{S_1}(S_1) = \frac{A_E}{B_E L} G_{0,2K}^{2\,K,0}\left(\frac{A_E S_1}{L} \middle| \begin{matrix} - \\ \{\alpha_{E_k} - 1\}_{k=1}^K, \{\beta_{E_k} - 1\}_{k=1}^K \end{matrix}\right) \tag{17}$$

$$f_{I_E}(I_E) = \sum_{kk=1}^{NN} \frac{\mathscr{A}_1 H_{kk} (-t_{kk})^{L-1} t_{kk}^{0.5}}{L} G_{0,2K}^{2K,0}\left(\mathscr{Z}_1 \middle| \begin{matrix} - \\ \{\alpha_{E_k} - 1\}_{k=1}^K, \{\beta_{E_k} - 1\}_{k=1}^K \end{matrix}\right) \tag{18}$$

$$f_{\gamma_E}(\gamma_E) = \sum_{kk=1}^{NN} \frac{\mathscr{A}_1 \mathscr{E}_1 H_{kk} t_{kk}^{0.5} (-t_{kk})^{L-1}}{2\sqrt{\bar{\gamma}\gamma_E}} G_{0,2K}^{2K,0}\left(\mathscr{Z}_2 \middle| \begin{matrix} - \\ \{\alpha_{E_k} - 1\}_{k=1}^K, \{\beta_{E_k} - 1\}_{k=1}^K \end{matrix}\right) \tag{19}$$

Integrating (24) by utilizing formula in [25, Eq. (07.34.21.0088.01)] the average BER is given by

$$P_E = \sum_{kk=1}^{NN} \frac{\delta \mathscr{A} \mathscr{E} L^b b^{\frac{2p+b-3}{2}} H_{kk} t_{kk}^{0.5} (-t_{kk})^{L-1}}{\Gamma(p)(\bar{\gamma})^{\frac{b}{2}} (2\pi)^{\frac{b+1}{2}} q^{\frac{b}{2}} (FA_0 I_a)^b} \times G_{2+2b,2+b}^{2,2+2b}\left(\frac{\mathscr{W}^2 b^b}{q^b} \middle| \begin{matrix} \frac{2i-2p-b}{2b}, \frac{2i-b}{2b}, -0.5, 0 \\ 0, 0.5, \frac{2i-b-2}{2b} \end{matrix}\right) \quad (25)$$

By utilizing [36, Eq. (22)] in (25), we get an asymptotic expression of average BER for High SNR, which is given in (26), shown at the bottom of the page.

In (26), $\mathscr{W} = \frac{L^b \mathscr{C} \exp(t_{kk} b)}{\bar{\gamma}^{\frac{b}{2}}}$, $\mathbb{A} = \left[\frac{2i-2p-b}{2b}, \frac{2i-b}{2b}, -0.5, 0\right]$, $\mathbb{B} = \left[0, 0.5, \frac{2i-b-2}{2b}\right]$ and $\mathbb{C} = [0, 0.5]$.

By considering only dominant terms in (26) the average BER asymptotic expression is given in (27), shown at the bottom of the page.

In (26), $\mathbb{C}_{min} = \min(\mathbb{C})$.

2) STRONG TURBULENCE

The average BER in case of strong turbulence is obtained by substituting (22) in (23) and integrating using formula [25, Eq.(07.34.21.0088.01)]. The obtained expression for average BER for strong turbulence is

$$P_E = \sum_{kk=1}^{NN} \frac{\mathscr{A}_1 \mathscr{E}_1 \delta 2^{u-2} H_{kk} t_{kk}^{0.5} (-t_{kk})^{L-1}}{\Gamma(p)(\bar{\gamma})^{\frac{1}{2}} (2\pi)^K q^{0.5}} \times G_{2,4K+1}^{4K,2}\left(\frac{\mathscr{W}_1{}^2}{q 2^{4K}} \middle| \begin{matrix} \frac{1-2p}{2}, 0.5 \\ \mathscr{O}, -0.5 \end{matrix}\right) \quad (28)$$

The asymptotic expression for average BER in case of strong turbulence for high SNR is given in (29), shown at the bottom of the page.

In (29), $\mathbb{D} = \left[\frac{1-2p}{2}, 0.5\right]$, $\mathbb{E} = \left[\frac{\{\alpha_{E_k}-1\}_{k=1}^K}{2}, \frac{\{\alpha_{E_k}\}_{k=1}^K}{2}, \frac{\{\beta_{E_k}-1\}_{k=1}^K}{2}, \frac{\{\beta_{E_k}\}_{k=1}^K}{2}, -0.5\right]$ and $\mathbb{F} = \left[\frac{\{\alpha_{E_k}-1\}_{k=1}^K}{2}, \frac{\{\alpha_{E_k}\}_{k=1}^K}{2}, \frac{\{\beta_{E_k}-1\}_{k=1}^K}{2}, \frac{\{\beta_{E_k}\}_{k=1}^K}{2}\right]$.

By considering only dominant terms in (29) the average BER asymptotic expression is given in (30), shown at the bottom of the page.

In (30), $\mathbb{F}_{min} = \min(\mathbb{F})$.

B. OUTAGE PROBABILITY

The outage probability (OP) of UVWOC MIMO EGC system for M number of sources and N number of detectors is given by [23]

$$O_E = \int_0^{\gamma_{th}} f_{\gamma_E}(\gamma_E)\, d\gamma_E = F_{\gamma_E}(\gamma_{th}) \quad (31)$$

where γ_{th} is SNR threshold.

1) WEAK TURBULENCE

By utilizing (21) in (31) the outage probability for weak turbulence can be written as

$$O_E = \sum_{kk=1}^{NN} \frac{\mathscr{A} \mathscr{E} L^b H_{kk} t_{kk}^{0.5} (-t_{kk})^{L-1} \gamma_{th}^{\frac{b}{2}}}{\pi b (\bar{\gamma})^{\frac{b}{2}} (FA_0 I_a)^b} \times G_{2+b,2+b}^{2,2+b}\left(\mathscr{W}^2 \gamma_{th}^b \middle| \begin{matrix} \frac{2i-b}{2b}, -0.5, 0 \\ 0, 0.5, \frac{2i-b-2}{2b} \end{matrix}\right) \quad (32)$$

The asymptotic expression for OP in case of weak turbulence is given in (33), as shown at the bottom of the next page, for high SNR.

In (33), $\mathbb{G} = \left[\frac{2i-b}{2b}, -0.5, 0\right]$, $\mathbb{H} = \left[0, 0.5, \frac{2i-b-2}{2b}\right]$ and $\mathbb{I} = [0, 0.5]$.

$$P_{E,asym} = \sum_{kk=1}^{NN} \frac{\delta \mathscr{A} \mathscr{E} L^b b^{\frac{2p+b-3}{2}} H_{kk} t_{kk}^{0.5} (-t_{kk})^{L-1}}{\Gamma(p)(\bar{\gamma})^{\frac{b}{2}} (2\pi)^{\frac{b+1}{2}} q^{\frac{b}{2}} (FA_0 I_a)^b} \sum_{k=1}^{2} \frac{\prod_{j=1, j\neq k}^{2} \Gamma\left(\mathbb{B}_j - \mathbb{C}_k\right) \prod_{j=1}^{2+2b} \Gamma\left(1 - \mathbb{A}_j + \mathbb{C}_k\right)}{\prod_{j=3}^{2+b} \Gamma\left(1 - \mathbb{B}_j + \mathbb{C}_k\right)} \left(\frac{\mathscr{W}^2 b^b}{q^b}\right)^{\mathbb{C}_k} \quad (26)$$

$$P_{E,asym} = \sum_{kk=1}^{NN} \frac{\delta \mathscr{A} \mathscr{E} L^b b^{\frac{2p+b-3}{2}} H_{kk} t_{kk}^{0.5} (-t_{kk})^{L-1}}{\Gamma(p)(\bar{\gamma})^{\frac{b}{2}} (2\pi)^{\frac{b+1}{2}} q^{\frac{b}{2}} (FA_0 I_a)^b} \frac{\prod_{\substack{j=1 \\ \mathbb{B}_j \neq \mathbb{C}_{min}}}^{2} \Gamma\left(\mathbb{B}_j - \mathbb{C}_{min}\right) \prod_{j=1}^{2+2b} \Gamma\left(1 - \mathbb{A}_j + \mathbb{C}_{min}\right)}{\prod_{j=3}^{2+b} \Gamma\left(1 - \mathbb{B}_j + \mathbb{C}_{min}\right)} \left(\frac{\mathscr{W}^2 b^b}{q^b}\right)^{\mathbb{C}_{min}} \quad (27)$$

$$P_{E,asym} = \sum_{kk=1}^{NN} \frac{\mathscr{A}_1 \mathscr{E}_1 \delta 2^{u-2} H_{kk} t_{kk}^{0.5} (-t_{kk})^{L-1}}{\Gamma(p)(\bar{\gamma})^{\frac{1}{2}} (2\pi)^K q^{0.5}} \sum_{k=1}^{4K} \frac{\prod_{\substack{j=1 \\ j\neq k}}^{4k} \Gamma\left(\mathbb{E}_j - \mathbb{F}_k\right) \prod_{j=1}^{2} \Gamma\left(1 - \mathbb{D}_j + \mathbb{F}_k\right)}{\Gamma(1.5 + \mathbb{F}_k)} \left(\frac{\mathscr{W}_1{}^2}{q 2^{4K}}\right)^{\mathbb{F}_k} \quad (29)$$

$$P_{E,asym} = \sum_{kk=1}^{NN} \frac{\mathscr{A}_1 \mathscr{E}_1 \delta 2^{u-2} H_{kk} t_{kk}^{0.5} (-t_{kk})^{L-1}}{\Gamma(p)(\bar{\gamma})^{\frac{1}{2}} (2\pi)^K q^{0.5}} \frac{\prod_{\substack{j=1 \\ \mathbb{E}_j \neq \mathbb{F}_{min}}}^{4k} \Gamma\left(\mathbb{E}_j - \mathbb{F}_{min}\right) \prod_{j=1}^{2} \Gamma\left(1 - \mathbb{D}_j + \mathbb{F}_{min}\right)}{\Gamma(1.5 + \mathbb{F}_{min})} \left(\frac{\mathscr{W}_1{}^2}{q 2^{4K}}\right)^{\mathbb{F}_{min}} \quad (30)$$

By considering only dominant terms in Eq. (12) the final OP aymptotic expression is expressed in (34), as shown at the bottom of the page. In (34), $\mathbb{I}_{min} = \min(\mathbb{I})$.

Beam spread function (BSF) represents the total scattered profile of incident optical beam. It shows the amount of light irradiance received as a function of distance of the receiver from the main beam axis at a particular link range.

The OP expression after including BSF function is given by

$$O_{E,BSF} = P_r(\gamma_{E,BSF} \leq \gamma_{th}) = \int_0^{\sqrt{\frac{4\gamma_{th}}{\pi\delta^2 BSF(\delta,d)\bar{\gamma}}}} f_{S_1}(S_1)dS_1 \tag{35}$$

where $\gamma_{E,BSF} = \frac{\pi\delta^2 BSF(\delta,d)S_1^2\bar{\gamma}}{4(MN)^2}$, δ is receiver point, d is link range, $BSF\ (\delta, d)$ is beam spread function for link range $d > 2\ m$ and $\delta < 2\ m$ is given in (36), as shown at the bottom of the next page, [37],

In (36) ${}_1F_2\ (-; -, -; -)$ is hyper geometric function, $P_{in}(\lambda)$ incident power, x_i is i^{th} root of Laguerre polynomial $L_n(x)$ of order n, and weight $W_i = \frac{x_i}{(n+1)^2(L_{n+1}(x_i))^2}$, $V_0(d)$ is variance of Gaussian source in free-space, $\mathcal{K} = \frac{1-g_1^2}{8\pi(1+g_1^2)^{3/2}}$, $g_1 = 0.924$ dominant forward scattering.

Substituting Eq. (13) in (35) and integrating resulting expression for OP is given as

$$O_{E,BSF} = b\exp(2a)\mathscr{J}_1 \times G_{1+b,1+b}^{1,1+b}\left(\exp(2a)\mathscr{J}_1 \middle| \begin{matrix} \frac{i-b}{b}, -1 \\ 0, \frac{i-b-1}{b} \end{matrix}\right) \tag{37}$$

where $\mathscr{J}_1 = \left(\frac{(MN))^2 4\gamma_{th}}{\pi\delta^2 BSF(\delta,d)\bar{\gamma}}\right)^{0.5b}$.

2) STRONG TURBULENCE

The outage probability of the MIMO UVWOC EGC system for strong turbulence can be obtained by substituting (22) in (31) and given as

$$O_E = \sum_{kk=1}^{NN} \frac{\mathscr{A}_1\mathscr{E}_1 2^u H_{kk} t_{kk}^{0.5}(-t_{kk})^{L-1}\sqrt{\gamma_{th}}}{2(2\pi)^K\sqrt{\bar{\gamma}}} \times G_{1,4K+1}^{4K,1}\left(\frac{\mathscr{W}_1^2\gamma_{th}}{2^{4K}} \middle| \begin{matrix} 0.5 \\ \mathscr{O}, -0.5 \end{matrix}\right) \tag{38}$$

The asymptotic expression of OP for High SNR is given in (39), as shown at the bottom of the next page.

In (39), $\mathbb{K} = \left[\frac{\{\alpha_{E_k}-1\}_{k=1}^K}{2}, \frac{\{\alpha_{E_k}\}_{k=1}^K}{2}, \frac{\{\beta_{E_k}-1\}_{k=1}^K}{2}, \frac{\{\beta_{E_k}\}_{k=1}^K}{2}, -0.5\right]$ and $\mathbb{L} = \left[\frac{\{\alpha_{E_k}-1\}_{k=1}^K}{2}, \frac{\{\alpha_{E_k}\}_{k=1}^K}{2}, \frac{\{\beta_{E_k}-1\}_{k=1}^K}{2}, \frac{\{\beta_{E_k}\}_{k=1}^K}{2}\right]$.

By considering only dominant terms in (39) the OP aymptotic expression is given in (40), as shown at the bottom of the next page. In (40), $\mathbb{L}_{min} = \min(\mathbb{L})$.

The OP expression for strong turbulence after adding BSF function is derived by substituting Eq. (17) in (35). After integration the resultant expression is given in (41) , as shown at the bottom of the next page.

C. ERGODIC CHANNEL CAPACITY

The ECC of the UVWOC MIMO EGC system is given by [15], [24]

$$C_E = \int_0^\infty \frac{1}{2}\log_2\left(1 + \frac{e\gamma_E}{2\pi}\right) f_{\gamma_E}(\gamma_E)\, d\gamma_E \tag{42}$$

where 'e' is the exponential constant.

1) WEAK TURBULENCE

In this section, we derive the ECC of weak turbulence condition by substituting (16) in (42). After substitution, the ECC is given by

$$C_E = \int_0^\infty \mathscr{P}_1 \log_2\left(1 + \frac{e\gamma_E}{2\pi}\right) G_{1,1}^{1,1}\left(\mathscr{Z} \middle| \begin{matrix} -1 \\ 0 \end{matrix}\right) d\gamma_E \tag{43}$$

where $\mathscr{P}_1 = \sum_{kk=1}^{NN} \frac{\mathscr{A}\mathscr{E}L^b H_{kk} t_{kk}^{0.5}(-t_{kk})^{L-1}\gamma_E^{(\frac{b}{2}-1)}}{4(\bar{\gamma})^{\frac{b}{2}}(FA_0I_a)^b}$. By using relation $\log_2(1+x) = 1.44\ G_{2,2}^{1,2}\left(x \middle| \begin{matrix} 1, 1 \\ 1, 0 \end{matrix}\right)$ in (43) and integrating it using formula in [22, Eq. (07.34.21.0013.01)] we get final ECC expression as

$$C_E = \sum_{kk=1}^{NN} \frac{1.44\mathscr{A}\mathscr{E}L^b H_{kk} t_{kk}^{0.5}(-t_{kk})^{L-1}}{b(2\pi e\bar{\gamma})^{\frac{b}{2}}(FA_0I_a)^b} \times G_{2+2b,2+2b}^{2+2b,2+b}\left(\frac{\mathscr{W}^2(2\pi)^b}{e^b} \middle| \begin{matrix} -0.5, 0, \frac{2i-b-2}{2b}, \frac{2i-b}{2b} \\ 0, 0.5, \frac{2i-b-2}{2b}, \frac{2i-b-2}{2b} \end{matrix}\right) \tag{44}$$

The asymptotic expression of ECC for weak turbulence regime is given in (45), as shown at the bottom of the next page.

$$O_{E,asym} = \sum_{kk=1}^{NN} \frac{\mathscr{A}\mathscr{E}L^b H_{kk} t_{kk}^{0.5}(-t_{kk})^{L-1}\gamma_{th}^{\frac{b}{2}}}{\pi b(\bar{\gamma})^{\frac{b}{2}}(FA_0I_a)^b} \sum_{k=1}^{2} \frac{\prod_{\substack{j=1 \\ j\neq k}}^{2}\Gamma\left(\mathbb{H}_j - \mathbb{I}_k\right)\prod_{j=1}^{2+b}\Gamma\left(1 - \mathbb{G}_j + \mathbb{I}_k\right)}{\prod_{j=3}^{2+b}\Gamma\left(1 - \mathbb{H}_j + \mathbb{I}_k\right)} \left(\mathscr{W}^2\gamma_{th}^b\right)^{\mathbb{I}_k} \tag{33}$$

$$O_{E,asym} = \sum_{kk=1}^{NN} \frac{\mathscr{A}\mathscr{E}L^b H_{kk} t_{kk}^{0.5}(-t_{kk})^{L-1}\gamma_{th}^{\frac{b}{2}}}{\pi b(\bar{\gamma})^{\frac{b}{2}}(FA_0I_a)^b} \frac{\prod_{\substack{j=1 \\ \mathbb{H}_j\neq\mathbb{I}_{min}}}^{2}\Gamma\left(\mathbb{H}_j - \mathbb{I}_{min}\right)\prod_{j=1}^{2+b}\Gamma\left(1 - \mathbb{G}_j + \mathbb{I}_{min}\right)}{\prod_{j=3}^{2+b}\Gamma\left(1 - \mathbb{H}_j + \mathbb{I}_{min}\right)} \left(\mathscr{W}^2\gamma_{th}^b\right)^{\mathbb{I}_{min}} \tag{34}$$

In (45), $\mathbb{M} = \left[-0.5, 0, \frac{2i-b-2}{2b}, \frac{2i-b}{2b}\right]$, $\mathbb{N} = \left[0, 0.5, \frac{2i-b-2}{2b}, \frac{2i-b-2}{2b}\right]$, $\mathbb{O} = \left[0, 0.5, \frac{2i-b-2}{2b}, \frac{2i-b-2}{2b}\right]$ and $\mathbb{O}_{min} = \min(\mathbb{O})$.

2) STRONG TURBULENCE

By following the same procedure as in (44) we can derive the ECC of a strong turbulence channel by substituting (19) in (42) and integrating it. The ECC of strong turbulence is given by

$$C_E = \sum_{kk=1}^{NN} \frac{1.44\mathscr{A}_1\mathscr{E}_1 2^u H_{kk} t_{kk}^{0.5}(-t_{kk})^{L-1}}{(2\pi)^{K+0.5}(e\bar{\gamma})^{0.5}} \times G_{2,4K+2}^{4K+2,1}\left(\frac{\mathscr{W}_1^2\pi}{e2^{4K-1}}\middle| \begin{matrix}-0.5, 0.5\\ \mathscr{O}, -0.5, -0.5\end{matrix}\right) \tag{46}$$

The asymptotic expression for ECC in case of strong turbulence for high SNR is given in (47), as shown at the bottom of the next page. In (47), $\mathbb{Q} = \left[\frac{\{\alpha_{E_k}-1\}_{k=1}^K}{2}, \frac{\{\alpha_{E_k}\}_{k=1}^K}{2}, \frac{\{\beta_{E_k}-1\}_{k=1}^K}{2}, \frac{\{\beta_{E_k}\}_{k=1}^K}{2}, -0.5, -0.5\right]$ $\mathbb{R} = \left[\frac{\{\alpha_{E_k}-1\}_{k=1}^K}{2}, \frac{\{\alpha_{E_k}\}_{k=1}^K}{2}, \frac{\{\beta_{E_k}-1\}_{k=1}^K}{2}, \frac{\{\beta_{E_k}\}_{k=1}^K}{2}, -0.5, -0.5\right]$ and $\mathbb{R}_{min} = \min(\mathbb{R})$.

V. RESULTS AND DISCUSSIONS

In this section, we have performed Monte Carlo simulations and numerical analysis of derived closed-form expressions quantifying the average BER, OP, and ECC of the UVWOC MIMO EGC system. The system parameters that we have considered for this computation are wavelength $\lambda = 530$ nm, extinction coefficient of ocean water $C(\lambda = 530\text{ nm}) = 0.056\,\text{m}^{-1}, A_0 = 1, g = 23.85,\ 2.65$ and 0.95 for weak, moderate and strong pointing error (PE) respectively [15], [26]. In this paper, we have considered a UVWOC link with transmitter–receiver separation with one, two, three, and four non-identical vertical layers where each layer has a thickness of 30 m. The critical parameters of the multi-layer UVWOC link, such as log amplitude variances and GG distribution parameters in case of weak turbulence (WT) and strong turbulence (ST), respectively, are presented in Table 4. This data has been drawn from studies conducted in the pacific ocean at high latitudes [7], [15].

Figs. 2 and 3 depicts the average BER performance of UVWOC MIMO EGC system in case of weak turbulence (WT) and strong turbulence (ST), respectively, for the different number of transmitters and receivers. We have assumed two vertical layers and weak PE. In Table 5, we have presented HTLN parameters of two vertical layers for different numbers of transmitters and receivers. The average SNR values and average SNR gain obtained with respect to OOK

$$BSF\,(\delta, d) = \frac{1}{2\pi}\sum_{i=1}^{n} W_i e^{x_i} P_{in}(\lambda)\exp\left(-\frac{V_0\,(d)\,x_i^2}{2}\right)\exp\left(-cd\right) \times\left(\exp\left(\frac{\mathcal{K}b\pi^2 d}{2}{}_1F_2\left(\frac{1}{2}; \frac{3}{2}, 2; -\frac{x_i d^2\pi^2}{4}\right) - \frac{0.6079b\mathcal{K}g_1 d}{1+g_1^2}\right) - 1\right) \tag{36}$$

$$O_{E,asym} = \sum_{kk=1}^{NN} \frac{\mathscr{A}_1\mathscr{E}_1 2^u H_{kk} t_{kk}^{0.5}(-t_{kk})^{L-1}\sqrt{\gamma_{th}}}{2(2\pi)^K\sqrt{\bar{\gamma}}} \sum_{k=1}^{4K} \frac{\prod_{\substack{j=1\\ j\neq k}}^{4k}\Gamma\left(\mathbb{K}_j - \mathbb{L}_k\right)\Gamma(0.5+\mathbb{L}_k)}{\Gamma(1.5+\mathbb{L}_k)}\left(\frac{\mathscr{W}_1^2\gamma_{th}}{2^{4K}}\right)^{\mathbb{L}_k} \tag{39}$$

$$O_{E,asym} = \sum_{kk=1}^{NN} \frac{\mathscr{A}_1\mathscr{E}_1 2^u H_{kk} t_{kk}^{0.5}(-t_{kk})^{L-1}\sqrt{\gamma_{th}}}{2(2\pi)^K\sqrt{\bar{\gamma}}} \frac{\prod_{\substack{j=1\\ \mathbb{K}_j\neq\mathbb{L}_{min}}}^{4k}\Gamma\left(\mathbb{K}_j - \mathbb{L}_{min}\right)\Gamma(0.5+\mathbb{L}_{min})}{\Gamma(1.5+\mathbb{L}_{min})}\left(\frac{\mathscr{W}_1^2\gamma_{th}}{2^{4K}}\right)^{\mathbb{L}_{min}} \tag{40}$$

$$O_{E,BSF} = \frac{A_E}{B_E}\sqrt{\frac{4\gamma_{th}}{\pi\delta^2 BSF(\delta,d)\bar{\gamma}}}\,G_{1,2K+1}^{2\,K,1}\left(A_E\sqrt{\frac{4\gamma_{th}}{\pi\delta^2 BSF(\delta,d)\bar{\gamma}}}\middle| \begin{matrix}0\\ \{\alpha_{E_k}-1\}_{k=1}^K, \{\beta_{E_k}-1\}_{k=1}^K, -1\end{matrix}\right) \tag{41}$$

$$C_{E,asym} = \sum_{kk=1}^{NN} \frac{1.44\mathscr{A}\mathscr{E}L^b H_{kk} t_{kk}^{0.5}(-t_{kk})^{L-1}}{b(2\pi e\bar{\gamma})^{\frac{b}{2}}(FA_0I_a)^b} \frac{\prod_{\substack{j=1\\ \mathbb{N}_j\neq\mathbb{O}_{min}}}^{2+2b}\Gamma\left(\mathbb{N}_j - \mathbb{O}_{min}\right)\prod_{j=1}^{2+b}\Gamma\left(1-\mathbb{M}_j+\mathbb{O}_{min}\right)}{\prod_{j=3+b}^{2+2b}\Gamma\left(\mathbb{M}_j - \mathbb{O}_{min}\right)}\left(\frac{\mathscr{W}^2(2\pi)^b}{e^b}\right)^{\mathbb{O}_{min}} \tag{45}$$

TABLE 4. Log-amplitude variances and GG parameters values for different numbers of vertical layers.

Number of vertical Layers	Total vertical link distance	Log-amplitude variance of each vertical layer	Total log-amplitude variance	GG parameters	
K	d (m)	$\sigma^2_{x_k}$	σ^2_t	α_k	β_k
1	30	9.26×10^{-2}	9.26×10^{-2}	3.99	1.81
2	60	9.26×10^{-2} 8.32×10^{-2}	17.59×10^{-2}	3.99 4.04	1.81 1.94
3	90	9.26×10^{-2} 8.32×10^{-2} 7.01×10^{-2}	24.59×10^{-2}	3.99 4.04 4.15	1.81 1.94 2.18
4	120	9.26×10^{-2} 8.32×10^{-2} 7.01×10^{-2} 5.57×10^{-2}	30.16×10^{-2}	3.99 4.04 4.15 4.41	1.81 1.94 2.18 2.58

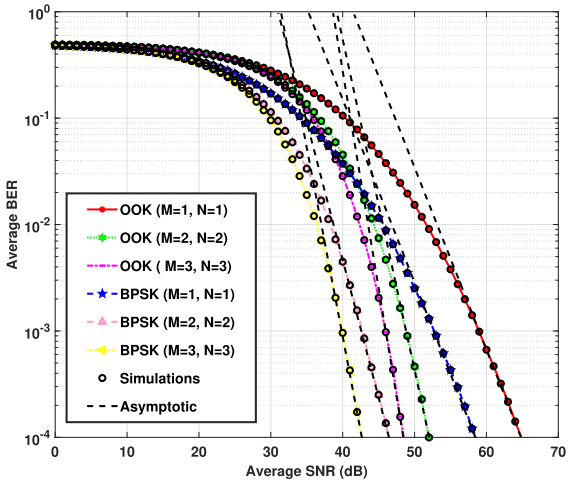

FIGURE 2. Average BER performance of UVWOC MIMO EGC system in case of weak turbulence regime for different numbers of transmitters and receivers.

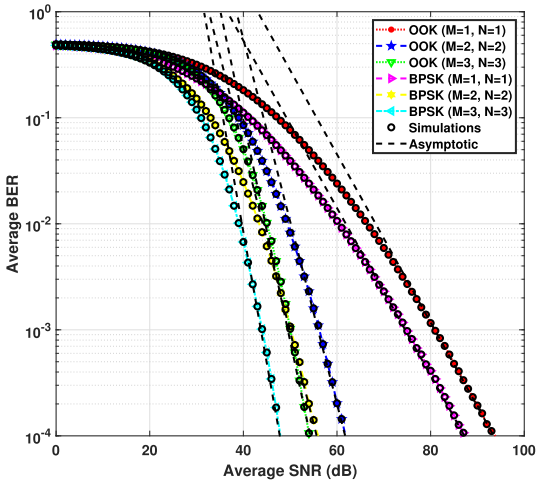

FIGURE 3. Average BER performance of UVWOC MIMO EGC system in case of strong turbulence regime for different numbers of transmitters and receivers.

modulation ($M = 1, N = 1$) to achieve an average BER of 10^{-4} for WT and ST are shown in Tables 6 and 7 respectively. It has been observed that the average SNR needed to achieve the same average BER (10^{-4}) decreases as the number of transmitters and receivers increases. In addition, the BPSK modulation is superior to OOK modulation for the same diversity order.

Figs. 4 and 5 depicts the average BER performance of two vertical layers of UVWOC MIMO EGC system perturbed by different pointing errors for weak turbulence and strong turbulence, respectively. We have considered two transmitters ($M = 2$) and two receivers ($N = 2$). It has been observed that the average BER performance deteriorates in the case of strong pointing errors (PE) for both weak and strong turbulence regimes.

TABLE 5. EGC Log-amplitude variances (σ^2_E) and means (μ_E) with corresponding HTLN parameters of two vertical layers for different numbers of transmitters (M) and detectors (N).

M	N	σ^2_E	μ_E	HTLN parameters	
				a	b
1	1	0.1759	-0.1759	0.39	2
2	2	0.0568	0.6364	-2.55	4
3	3	0.0268	1.0718	-5.36	5

In Figs. 6 and 7 we have presented the average BER performance of the UVWOC MIMO EGC system by varying vertical layers from one to four for WT and ST, respectively. We have assumed weak PE and considered transmitters and receivers three each ($M = 3, N = 3$). In Table 8, we have presented HTLN parameters of different vertical layers for $M = 3$ and $N = 3$ EGC system. It has been observed from

$$C_{E,asym} = \sum_{kk=1}^{NN} \frac{1.44\mathscr{A}_1\mathscr{E}_1 2^u H_{kk} t_{kk}^{0.5}(-t_{kk})^{L-1}}{(2\pi)^{K+0.5}(e\bar{\gamma})^{0.5}} \frac{\prod_{\substack{j=1 \\ \mathbb{Q}_j \neq \mathbb{R}_{min}}}^{4K+2} \Gamma\left(\mathbb{Q}_j - \mathbb{R}_{min}\right)\Gamma(1.5 + \mathbb{R}_{min})}{\Gamma(0.5 - \mathbb{R}_{min})} \left(\frac{\mathscr{W}_1^2 \pi}{e 2^{4K-1}}\right)^{\mathbb{R}_{min}} \tag{47}$$

TABLE 6. Average SNR values and gain to achieve average BER of 10^{-4} for different numbers of transmitters and receivers in case of WT.

M	N	Average SNR (dB)		Average SNR gain (dB)	
		OOK	BPSK	OOK	BPSK
1	1	64	58	0	6
2	2	52	46	12	18
3	3	48	42	16	22

TABLE 7. Average SNR values and gain to achieve average BER of 10^{-4} for different numbers of transmitters and receivers in case of ST.

M	N	Average SNR (dB)		Average SNR gain (dB)	
		OOK	BPSK	OOK	BPSK
1	1	93	87	0	6
2	2	61	55	32	38
3	3	54	47	39	46

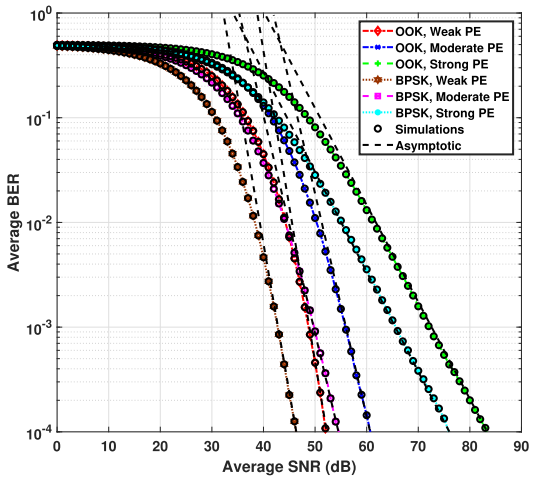

FIGURE 4. Average BER performance of UVWOC MIMO EGC system (M=2, N=2) in case of weak turbulence regime for different pointing errors.

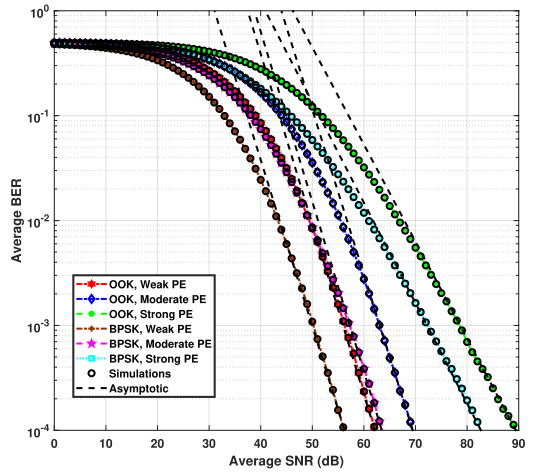

FIGURE 5. Average BER performance of UVWOC MIMO EGC system (M=2, N=2) in case of strong turbulence regime for different pointing errors.

Figs. 6 and 7, the average BER performance decreases as the number of vertical layers increases in both cases.

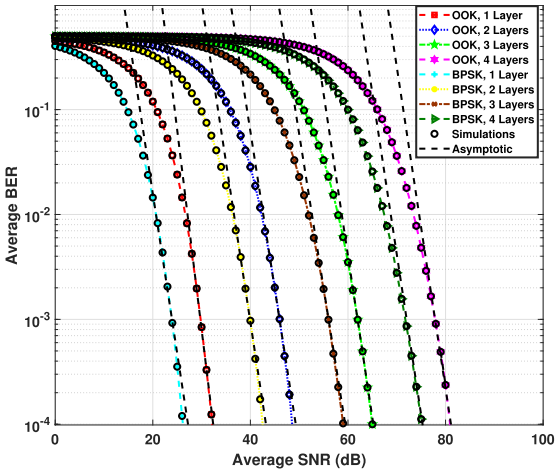

FIGURE 6. Average BER performance of UVWOC MIMO EGC system ($M = 3, N = 3$) in case of weak turbulence regime for a different number of vertical layers.

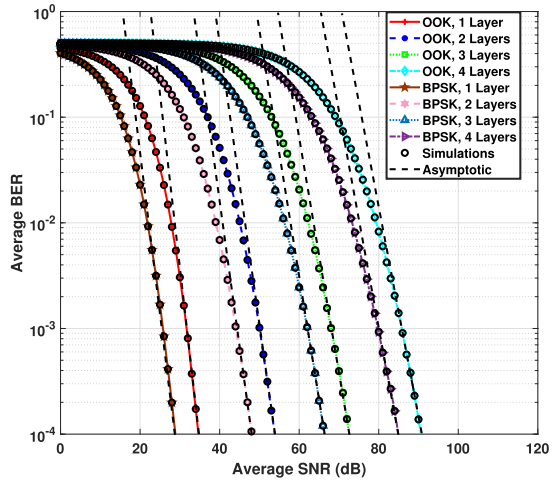

FIGURE 7. Average BER performance of UVWOC MIMO EGC system ($M = 3, N = 3$) in case of strong turbulence regime for a different number of vertical layers.

TABLE 8. EGC variances (σ_E^2) and means (μ_E^2) with corresponding HTLN parameters for transmitters ($M = 3$) and receivers ($N = 3$).

K	σ_E^2	μ_E^2	HTLN parameters	
			a	b
1	1.0865	0.0122	-8.69	8
2	1.0718	0.0268	-5.36	5
3	1.0557	0.0429	-4.22	4
4	1.0405	0.0581	-4.16	4

Closed-form expressions for vertical link performance, quantifying the average bit error rate (BER) for receive diversity schemes such as selection combining (SC) and maximum ratio combining (MRC), were derived in [15]. These expressions account for the impact of pointing errors, particularly within a regime of weak turbulence. In Fig 8, we have provided the simulation results of average BER for various receive diversity schemes (EGC, MRC, and SC) in

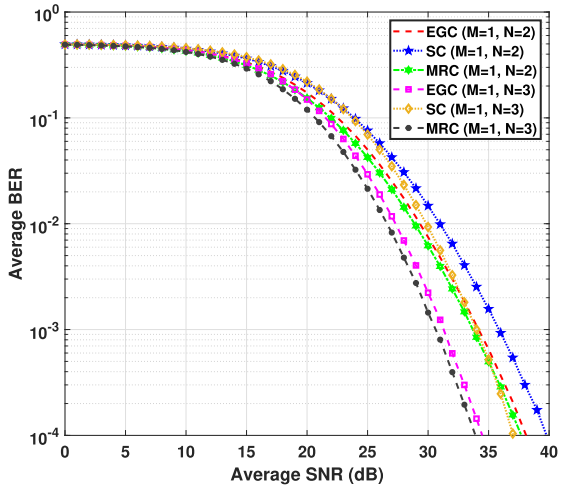

FIGURE 8. Receive diversity schemes.

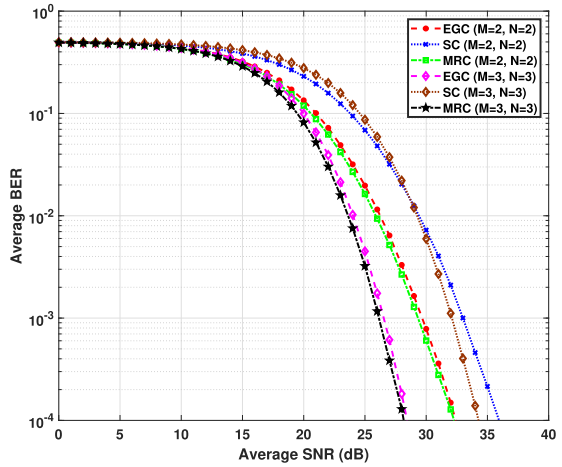

FIGURE 9. Monte-carlo simulations for different MIMO schemes.

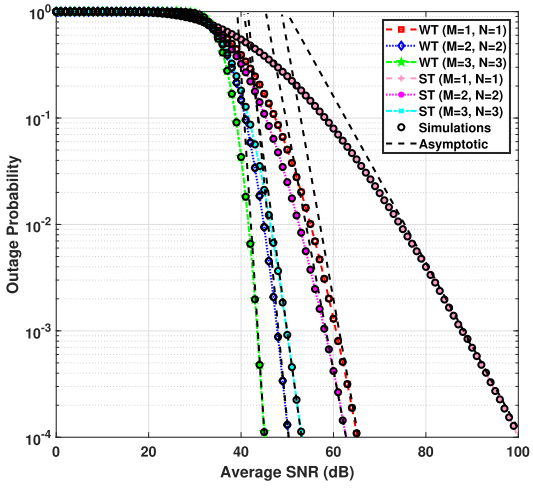

FIGURE 10. Outage Probability of UVWOC MIMO EGC system for different numbers of transmitters and receivers.

TABLE 9. Average SNR values and average SNR gains to achieve OP of 10^{-4} for different numbers of transmitters and receivers in case of WT.

M	N	Average SNR (dB)	Average SNR gain (dB)
1	1	65	0
2	2	50	15
3	3	45	20

TABLE 10. Average SNR values and average SNR gains to achieve OP of 10^{-4} for different numbers of transmitters and receivers in case of ST.

M	N	Average SNR (dB)	Average SNR gain (dB)
1	1	100	0
2	2	62	38
3	3	53	47

the case of a vertical link. Here we have considered weak turbulence and weak pointing error for two vertical layers (K=2). From Fig. 8, it is evident that EGC is better than SC regarding average SNR gain. An average SNR gain of 5dB is observed from Fig. 8 compared to SC of the same diversity order. In addition, the performance of EGC is approximately equal to MRC. We also have provided the monte carlo simulations of different MIMO technologies in Fig. 9. Here we have considered weak turbulence and weak pointing error for two vertical layers. It is evident from Fig. 9 there will be no significant gain when MRC is compared with EGC. The performance of MIMO-EGC is better than SC.

In Fig. 10, the outage probability of UVWOC MIMO EGC for different numbers of transmitters and receivers has been computed and simulated by considering two vertical layers. Here we have considered SNR threshold $\gamma_{th} = 5$ dB, weak PE for weak and strong turbulence conditions. The average SNR values and average gain obtained with respect to single input single output ($M = 1$, $N = 1$) for the outage probability of 10^{-4} in case of WT and ST are shown in Tables 9 and 10 respectively. It has been observed that an increase in the number of transmitters and receivers decreases outage probability and hence improves the performance of the system.

In Fig. 11, the outage probability of weak turbulence and strong turbulence for different SNR thresholds (γ_{th}) are computed and simulated. We have considered two vertical layers with weak PE, $M = 2$ and $N = 2$. It has been observed from Fig. 11 that as the SNR threshold increases, the OP increases, which deteriorates the performance of the UVWOC MIMO EGC system.

In Fig. 12, the OP for weak, moderate, and strong PE are plotted for weak and strong turbulence regimes. Here we have taken $M = 3$ and $N = 3$ for two vertical layers of underwater medium. The SNR threshold $\gamma_{th} = 5$ dB is assumed. The result shows that to achieve OP of 10^{-4}, the average SNR required is 45 dB for weak PE, 52 dB for moderate PE, and 68 dB for strong PE in case of weak turbulence. The corresponding values of average SNR are 52 dB for weak PE, 62 dB for moderate PE, and 73 dB for strong PE, respectively, under the strong turbulence regime. From this figure, it can be inferred that as PE increases, the average SNR required to establish a given OP increases.

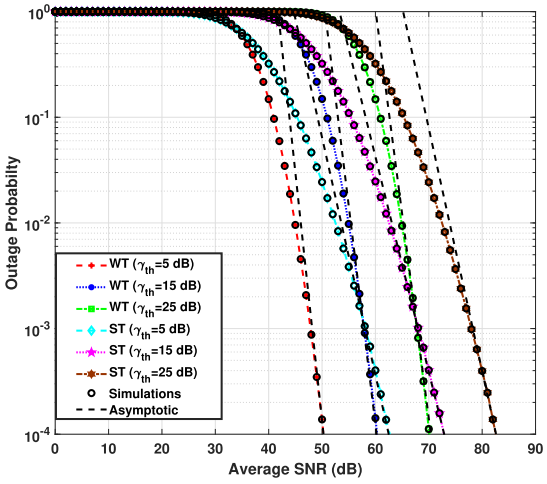

FIGURE 11. Outage Probability of UVWOC MIMO EGC ($M = 2, N = 2$) system for different SNR thresholds (γ_{th}).

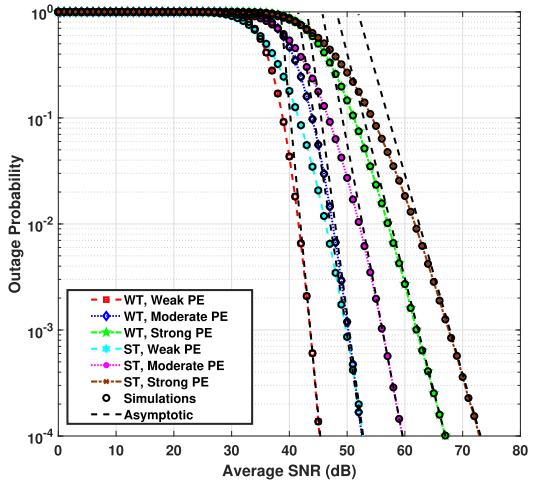

FIGURE 12. Outage Probability of UVWOC MIMO EGC ($M = 3, N = 3$) system for different pointing errors.

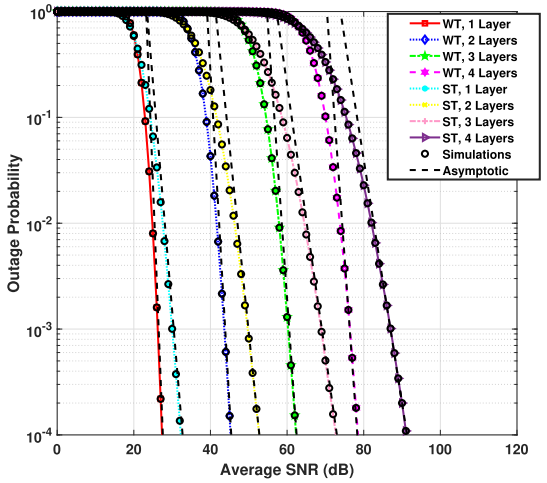

FIGURE 13. Outage Probability of UVWOC MIMO EGC ($M = 3, N = 3$) system for different number of vertical layers.

In Fig. 13, the OP values corresponding to different numbers of vertical layers are presented. Here we have considered

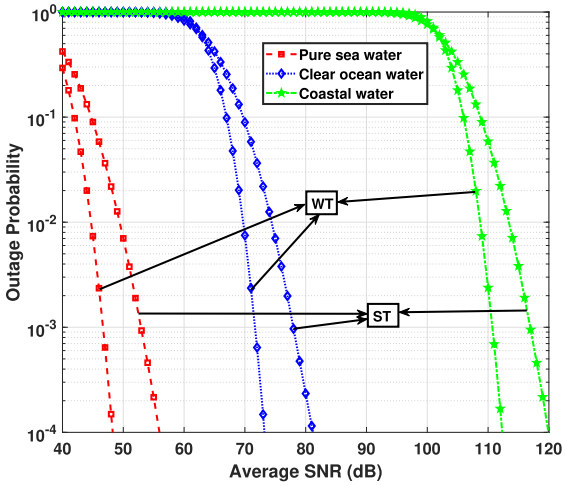

FIGURE 14. Outage Probability of UVWOC MIMO EGC ($M = 3, N = 3$) system for different water types.

weak PE, $\gamma_{th} = 5$ dB and transmitter-receiver ($M = 3$, $N = 3$). It can be inferred from a study of this plot that the SNR required to establish a given value of OP increases as the number of vertical layers is increased.

In Fig. 14, we calculated the OP values using the BSF function for various water types. The calculations were performed with a fixed δ value of 20 cm and specific BSF values: -18 dB, -43 dB, and -82 dB, corresponding to pure sea water, clear ocean water, and coastal water, as referenced in [37]. Our observations from the figure reveal that, as the turbidity of the water increases, there is a noticeable elevation in the average signal-to-noise ratio (SNR) required to attain the same OP of 10^{-4} for both WT and ST conditions. Specifically, a significant average SNR improvement of 64 dB and 39 dB is evident for pure and clear ocean water, respectively, when compared with the performance in coastal for both WT and ST.

In Fig. 15, we present the ECC of UVWOC MIMO EGC for differing numbers of transmitters and receivers. In this computation, we have considered two vertical layers of underwater medium influenced by weak PE. It is observed that an increase in the number of transmitters and receivers results in an improvement in the ECC. The ECC values which have been determined at an average SNR of 70 dB, are presented in Table 11.

In Fig. 16, we present the ECC of UVWOC MIMO EGC for different PE regimes under the influence of weak and strong turbulence regimes. Here we have considered two transmitters and two receivers ($M = 2, N = 2$) and two vertical layers of underwater medium. It has been observed as PE increases, there is a reduction in the value of ECC value for both weak and strong turbulence regimes. The ECC values determined at an average SNR value of 70 dB are shown in Table 12.

Fig. 17 depicts the ECC values for different numbers of vertical layers. Here we have considered weak PE regime and

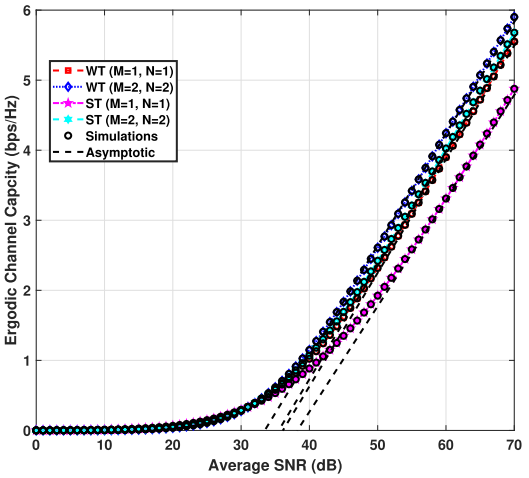

FIGURE 15. Ergodic channel capacity of UVWOC MIMO EGC system for different number of transmitters and receivers.

TABLE 11. ECC values to achieve average SNR of 70 dB for different numbers of transmitters and receivers.

M	N	Turbulence	ECC (bps/Hz)
1	1	Weak	5.54
2	2	Weak	5.91
1	1	Strong	4.87
2	2	Strong	5.67

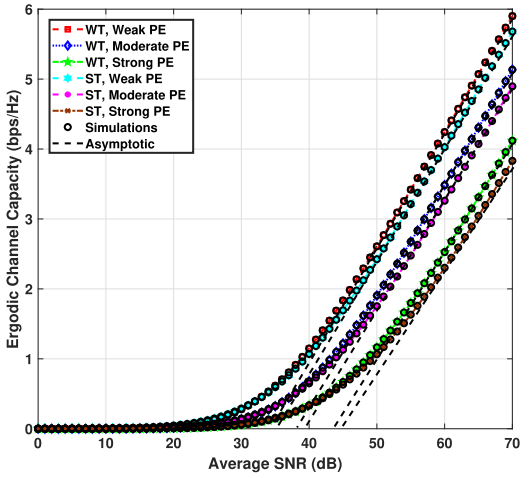

FIGURE 16. Ergodic channel capacity of UVWOC MIMO EGC ($M = 2$, $N = 2$) system for different pointing errors.

TABLE 12. ECC values for an average SNR of 70 dB.

PE	ECC for WT (bps/Hz)	ECC for ST (bps/Hz)
Weak	5.91	5.67
Moderate	5.13	4.90
Strong	4.12	3.83

transmitter-receiver combination as ($M = 3, N = 3$). It is observed from Fig. 17 that the ECC value decreases as the number of the vertical layer increases from one to four.

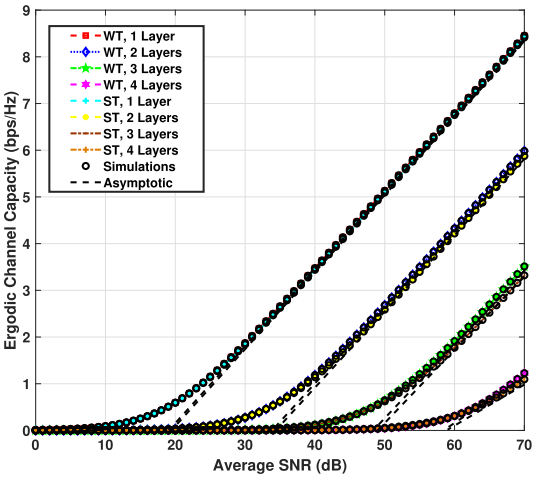

FIGURE 17. Ergodic channel capacity of UVWOC MIMO EGC ($M = 3$, $N = 3$) system for different number of vertical layers.

VI. CONCLUSION

In this paper, we have investigated the performance of a UVWOC link employing a MIMO EGC scheme perturbed by weak and strong underwater turbulence under the influence of pointing errors and attenuation losses. We have derived closed-form expressions for the average BER, OP, and ECC, considering the different numbers of transmitters and receivers. The average BER supported by the vertical link has been determined for different modulation schemes, differing numbers of vertical layers, and differing degrees of pointing error. From the results obtained in the paper, we have concluded that as diversity order increases, the average BER performance improves. In addition, BPSK modulation is superior to OOK modulation in terms of improvement in average BER for the same diversity order. Further, closed-form expressions for the OP and ECC have been derived for the UVWOC MIMO EGC system. The OP has been analyzed for different SNR thresholds, distinct ocean water types, differing numbers of vertical layers, and pointing errors. We conclude that there is a reduction in the average SNR requirement as the number of transmitters and receivers increases. The plots obtained by computation using the analytic closed-form expressions derived by us correspond very closely to the plots obtained using Monte-Carlo simulation.

REFERENCES

[1] M. C. Domingo, "An overview of the Internet of Underwater Things," *J. Netw. Comput. Appl.*, vol. 35, no. 6, pp. 1879–1890, 2012.
[2] P. Krishnan, "Performance analysis of hybrid RF/FSO system using BPSK-SIM and DPSK-SIM over gamma-gamma turbulence channel with pointing errors for smart city applications," *IEEE Access*, vol. 6, pp. 75025–75032, 2018.
[3] H. Kaushal and G. Kaddoum, "Underwater optical wireless communication," *IEEE Access*, vol. 4, pp. 1518–1547, 2016.
[4] P. N. Ramavath, S. A. Udupi, and P. Krishnan, "Experimental demonstration and analysis of underwater wireless optical communication link: Design, BCH coded receiver diversity over the turbid and turbulent seawater channels," *Microw. Opt. Technol. Lett.*, vol. 62, no. 6, pp. 2207–2216, Jun. 2020.

[5] B. K. Levidala, P. N. Ramavath, and P. Krishnan, "High-speed long-range multihop underwater wireless optical communication convergent with free-space optical system for optical Internet of Underwater Things and underwater optical wireless sensor network applications," *Opt. Eng.*, vol. 61, no. 7, Jul. 2022, Art. no. 076107.
[6] R. Chester and T. D. Jickells, *Marine Geochemistry: Chester/Marine Geochemistry,* 3rd ed. Nashville, TN, USA: Wiley, 2012.
[7] M. Elamassie and M. Uysal, "Vertical underwater visible light communication links: Channel modeling and performance analysis," *IEEE Trans. Wireless Commun.*, vol. 19, no. 10, pp. 6948–6959, Oct. 2020.
[8] P. N. Ramavath, S. A. Udupi, and P. Krishnan, "High-speed and reliable underwater wireless optical communication system using multiple-input multiple-output and channel coding techniques for IoUT applications," *Opt. Commun.*, vol. 461, Apr. 2020, Art. no. 125229.
[9] P. N. Ramavath, S. A. Udupi, and P. Krishnan, "Co-operative RF-UWOC link performance over hyperbolic tangent log-normal distribution channel with pointing errors," *Opt. Commun.*, vol. 469, Aug. 2020, Art. no. 125774.
[10] Z. Lin, G. Xu, Q. Zhang, and Z. Song, "Average symbol error probability and channel capacity of the underwater wireless optical communication systems over oceanic turbulence with pointing error impairments," *Opt. Exp.*, vol. 30, no. 9, pp. 15327–15343, 2022.
[11] R. Boluda-Ruiz, A. GarcaZambrana, B. CastilloVzquez, and S. Hranilovic, "Impact of angular pointing error on BER performance of underwater optical wireless links," *Opt. Exp.*, vol. 28, no. 23, pp. 34606–34622, 2020.
[12] M. V. Jamali, J. A. Salehi, and F. Akhoundi, "Performance studies of underwater wireless optical communication systems with spatial diversity: MIMO scheme," *IEEE Trans. Commun.*, vol. 65, no. 3, pp. 1176–1192, Mar. 2017.
[13] W. O. Popoola, Z. Ghassemlooy, S. Gao, J. I. H. Allen, and E. Leitgeb, "Free-space optical communication employing subcarrier modulation and spatial diversity in atmospheric turbulence channel," *IET Optoelectron.*, vol. 2, no. 1, pp. 16–23, Feb. 2008.
[14] N. I. Miridakis, M. Matthaiou, and G. K. Karagiannidis, "Multiuser relaying over mixed RF/FSO links," *IEEE Trans. Commun.*, vol. 62, no. 5, pp. 1634–1645, May 2014.
[15] C. S. S. Shetty, R. P. Naik, U. S. Acharya, and W.-Y. Chung, "Performance analysis of underwater vertical wireless optical communication system in the presence of weak turbulence, pointing errors and attenuation losses," *Opt. Quantum Electron.*, vol. 55, no. 1, p. 1, Jan. 2023.
[16] M. R. Bhatnagar and Z. Ghassemlooy, "Performance analysis of gamma–gamma fading FSO MIMO links with pointing errors," *J. Lightw. Technol.*, vol. 34, no. 9, pp. 2158–2169, 2016.
[17] A. A. Farid and S. Hranilovic, "Outage capacity optimization for free-space optical links with pointing errors," *J. Lightw. Technol.*, vol. 2, no. 7, pp. 1702–1710, Jul. 2007.
[18] M. Miao and X. Li, "Novel approximate distribution of the sum of gamma–gamma variates with pointing errors and applications in MIMO FSO links," *Opt. Commun.*, vol. 486, May 2021, Art. no. 126780.
[19] N. D. Chatzidiamantis and G. K. Karagiannidis, "On the distribution of the sum of gamma-gamma variates and applications in RF and optical wireless communications," *IEEE Trans. Commun.*, vol. 59, no. 5, pp. 1298–1308, May 2011.
[20] Wolfram.com. *Meijer G-Function: Integration (Formula 07.34.21.0084)*. Accessed: Jul. 11, 2023. [Online]. Available: http://functions.wolfram.com/07.34.21.0084.01
[21] E. Zedini, H. Soury, and M.-S. Alouini, "Dual-hop FSO transmission systems over gamma–gamma turbulence with pointing errors," *IEEE Trans. Wireless Commun.*, vol. 16, no. 2, pp. 784–796, Feb. 2017.
[22] Wolfram.com. *Meijer G-Function: Integration (Formula 07.34.21.0013)*. Accessed: Jul. 11, 2023. [Online]. Available: http://functions.wolfram.com/07.34.21.0013.01
[23] L. B. Kumar, R. P. Naik, P. Krishnan, A. A. B. Raj, A. K. Majumdar, and W.-Y. Chung, "RIS assisted triple-hop RF-FSO convergent with UWOC system," *IEEE Access*, vol. 10, pp. 66564–66575, 2022.
[24] I. S. Ansari, M.-S. Alouini, and J. Cheng, "Ergodic capacity analysis of free-space optical links with nonzero boresight pointing errors," *IEEE Trans. Wireless Commun.*, vol. 14, no. 8, pp. 4248–4264, Aug. 2015.
[25] Wolfram.com. *Meijer G-Function: Integration (Formula 07.34.21.0088)*. Accessed: Jul. 11, 2023. [Online]. Available: http://functions.wolfram.com/07.34.21.0088.01
[26] M. Elamassie, F. Miramirkhani, and M. Uysal, "Performance characterization of underwater visible light communication," *IEEE Trans. Commun.*, vol. 67, no. 1, pp. 543–552, Jan. 2019.
[27] M. Elamassie, S. M. Sait, and M. Uysal, "Underwater visible light communications in cascaded gamma-gamma turbulence," in *Proc. IEEE Globecom Workshops (GC Wkshps)*, Dec. 2018, pp. 1–6.
[28] A. Yilmaz, M. Elamassie, and M. Uysal, "Diversity gain analysis of underwater vertical MIMO VLC links in the presence of turbulence," in *Proc. IEEE Int. Black Sea Conf. Commun. Netw. (BlackSeaCom)*, Jun. 2019, pp. 1–6.
[29] P. Concus, D. Cassatt, G. Jaehnig, and E. Melby, "Tables for the evaluation of $\int_0^\infty x^\beta e^{-x} f(x)dx$ by Gauss–Laguerre quadrature," *Math. Comput.*, vol. 17, no. 83, p. 245, 1963.
[30] M. Elamassie and M. Uysal, "Vertical underwater VLC links over cascaded gamma-gamma turbulence channels with pointing errors," in *Proc. IEEE Int. Black Sea Conf. Commun. Netw. (BlackSeaCom)*, Jun. 2019, pp. 1–5.
[31] I. C. Ijeh, M. A. Khalighi, M. Elamassie, S. Hranilovic, and M. Uysal, "Outage probability analysis of a vertical underwater wireless optical link subject to oceanic turbulence and pointing errors," *J. Opt. Commun. Netw.*, vol. 14, no. 6, pp. 439–453, Jun. 2022.
[32] M. V. Jamali, A. Chizari, and J. A. Salehi, "Performance analysis of multi-hop underwater wireless optical communication systems," *IEEE Photon. Technol. Lett.*, vol. 29, no. 5, pp. 462–465, Mar. 1, 2017.
[33] M. V. Jamali, A. Mirani, A. Parsay, B. Abolhassani, P. Nabavi, A. Chizari, P. Khorramshahi, S. Abdollahramezani, and J. A. Salehi, "Statistical studies of fading in underwater wireless optical channels in the presence of air bubble, temperature, and salinity random variations," *IEEE Trans. Commun.*, vol. 66, no. 10, pp. 4706–4723, Oct. 2018.
[34] M. V. Jamali, P. Nabavi, and J. A. Salehi, "MIMO underwater visible light communications: Comprehensive channel study, performance analysis, and multiple-symbol detection," *IEEE Trans. Veh. Technol.*, vol. 67, no. 9, pp. 8223–8237, Sep. 2018.
[35] S. M. Navidpour, M. Uysal, and M. Kavehrad, "BER performance of free-space optical transmission with spatial diversity," *IEEE Trans. Wireless Commun.*, vol. 6, no. 8, pp. 2813–2819, Aug. 2007.
[36] R. P. Naik and W.-Y. Chung, "Evaluation of reconfigurable intelligent surface-assisted underwater wireless optical communication system," *J. Lightw. Technol.*, vol. 40, no. 13, pp. 4257–4267, Jul. 1, 2022.
[37] P. Saxena and M. R. Bhatnagar, "A simplified form of beam spread function in underwater wireless optical communication and its applications," *IEEE Access*, vol. 7, pp. 105298–105313, 2019.
[38] P. Saxena, A. Mathur, and M. R. Bhatnagar, "BER performance of an optically pre-amplified FSO system under turbulence and pointing errors with ASE noise," *J. Opt. Commun. Netw.*, vol. 9, no. 6, pp. 498–510, Jun. 2017.

C. S. SAVIDHAN SHETTY (Student Member, IEEE) received the master's degree from Visvesvaraya Technological University, Karnataka, India. He is currently pursuing the Ph.D. degree with the Department of Electronics and Communication Engineering, National Institute of Technology Karnataka, Surathkal, India. His research interests include RF wireless communication, free-space optical communication, and underwater optical wireless communication.

RAMAVATH PRASAD NAIK received the M.Tech. degree from the Department of Electronics and Communication Engineering, Motilal Nehru National Institute of Technology Allahabad, in 2015, and the Ph.D. degree from the National Institute of Technology Karnataka, Surathkal, in 2021. He was a Postdoctoral Researcher from September 2021 to January 2023 and a Research Professor from February 2023 to April 2023 with the Research Institute of Artificial Intelligence Convergence, Pukyong National University, Busan, Republic of Korea. He is currently an Assistant Professor with the Department of Electronics and Communication Engineering, National Institute of Technology Rourkela, Odisha, India. His research interests include free-space and underwater optical wireless communication, theory and application of error control codes, and cooperative communication.

U. SHRIPATHI ACHARYA (Senior Member, IEEE) received the Ph.D. degree in the area of error control codes and their application in wireless communication from the Indian Institute of Science, in 2005. He has led several funded research projects in the area of wireless communication, free space optical communication, and professional electronics. He is a Professor with the Department of Electronics and Communication, National Institute of Technology Karnataka. His areas of interest are the application of error control codes to communication and data storage, underwater free space communication, wireless and MIMO communication, and professions electronics. He is a fellow of the Institution of Engineers (India).

WAN-YOUNG CHUNG (Senior Member, IEEE) received the B.Eng. and master's degrees in electronic engineering from Kyungpook National University, Daegu, South Korea, in 1987 and 1989, respectively, and the Ph.D. degree in sensor engineering from Kyushu University, Fukuoka, Japan, in 1998. From 1999 to 2008, he was an Associate Professor at Dongseo University, Busan, South Korea. He is currently a Professor with the Department of Electronic Engineering, Pukyong National University, Busan. His research interests include wireless sensor networks, ubiquitous healthcare and automobile applications, smart light-emitting systems with visible light communication, and embedded systems. He is the Educational and Research Group Leader of Artificial Intelligence Convergence, which is supported by the Brain Korea 21 (BK21) Four Project.